

PAPER • OPEN ACCESS

Design and analysis of an electric tiltrotor unmanned aerial vehicle

To cite this article: Ahmed A Gebрил and Ashraf M Kamal 2023 *J. Phys.: Conf. Ser.* **2616** 012008

View the [article online](#) for updates and enhancements.

You may also like

- [Research on the Application of Small Area 3D Modeling Based on Consumer UAV—Take DJI Yu-2 UAV as an Example](#)
Zhan Teng, Wanqing Liu and Yaowu Yi
- [Communication Energy Optimization of UAV-assisted WSN Data Transmission](#)
Hao Liu, Renwen Chen, Zihao Jiang et al.
- [Design of UAV wireless communication system](#)
Xinyue Bai

PRIME
PACIFIC RIM MEETING
ON ELECTROCHEMICAL
AND SOLID STATE SCIENCE

HONOLULU, HI
Oct 6–11, 2024

Abstract submission deadline:
April 12, 2024

Learn more and submit!

Joint Meeting of
The Electrochemical Society
•
The Electrochemical Society of Japan
•
Korea Electrochemical Society

Design and analysis of an electric tiltrotor unmanned aerial vehicle

Ahmed A Gebri¹ and Ashraf M Kamal²

¹ B.Sc., Aircraft Mechanics Department, Military Technical College, Cairo, Egypt.

² Assistant Professor, Aircraft Mechanics Department, Military Technical College, Cairo, Egypt.

E-mail: engaash9@gmail.com

Abstract. The concept of tiltrotor aircraft has been around for over seventy years, but it was not until the last decade that the advancement in Unmanned Aerial Vehicle (UAV) technology has made them a viable option. Although the design requirements of such UAV are complex and require careful consideration, the potential benefits are significant. Motivated by their potential capabilities, this paper aims to present a complete procedure for designing an electric tiltrotor UAV that incorporates the attributes of both fixed and rotary wing aircraft, including all necessary mathematical formulations. The paper explores the diverse aspects of the design and analysis of tiltrotor UAVs, from conceptual, preliminary, and detail design to aerodynamics, performance, and stability analysis. The detailed weight analysis is performed using six different methods from different references to assess their applicability for use with electric tiltrotor UAV. After designing and selecting the UAV components, an iteration process is performed to check and resize the estimated design parameters.

1. Introduction

In recent years, unmanned aerial vehicles (UAVs) have become increasingly popular and broadly used in both military and civilian applications due to their ability to perform a variety of tasks with minimal human intervention. These UAVs are divided into two main categories: fixed-wing UAVs and rotary-wing UAVs and each type has their own advantages and disadvantages. Transitional UAVs are a type of UAV that combines the benefits of both fixed-wing and rotary-wing aircraft, allowing them to take off and land vertically like a helicopter while also having the speed and range of a fixed-wing aircraft. These transitional UAVs offer many advantages over conventional UAVs, including increased efficiency, greater maneuverability, and improved safety. Transitional UAVs are divided into two types: convertiplanes and tail-sitters. A convertiplane (e.g., tiltrotor, tiltwing, rotor-wings, and dual systems) keeps its airframe in the same position during all flight modes, and different transition mechanisms are used to obtain cruise flight mode. On the other hand, a tail-sitter is an aircraft that launches and lands vertically on its tail, requiring the whole airframe to tilt in order to achieve cruise flight (e.g., mono thrust transitioning, collective thrust transitioning, and differential thrust transitioning). Figure 1 shows the configurations of some of these transitional UAVs.

Among the different transitional types, the tilt rotor UAV is the most popular one. Tiltrotor UAVs typically have two/more rotors that can be tilted from vertical to horizontal positions for take-off and landing. This allows the tiltrotor UAV to hover, take off and land vertically like a helicopter while also having the speed and range of a fixed-wing aircraft. Tilt rotor UAVs are ideal for applications such as search and rescue operations, surveillance missions, aerial photography, or delivering supplies in difficult terrain. They are also more efficient than traditional helicopters due to their ability to transition from vertical flight to horizontal flight quickly.



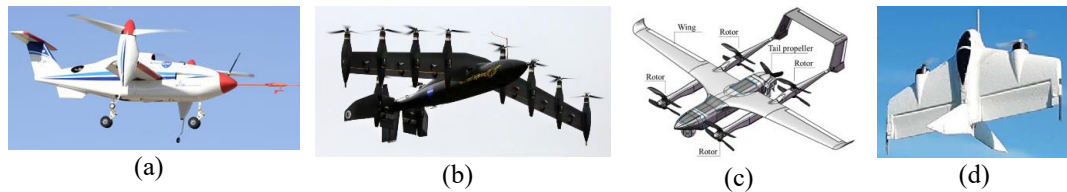


Figure 1. Tiltrotor, tilt-wing, dual-system, and tail-sitter UAVs, respectively.

The main goal of this paper is to perform the design and aerodynamic/performance analysis of an electric transitional UAV that satisfies the design requirements in Table 1. Additionally, the designed UAV should satisfy modular design, easy and rapid production and assembly, compact in transportation with low manufacturing cost.

Table 1 Performance and weight design requirements for the transitional UAV

Specification	Value	Specification	Value
Payload weight	3.5 kg	Cruise speed	22-25 m/s
Ceiling in fixed wing mode	3 km	Take-off and landing method	VTOL
Vmax in FW Flight mode	35 m/s	Transition time	≤ 8 s
Range in FW Flight Mode	50 km	ROC at VTOL flight mode	3 m/s
Rate of climb in FW	4 m/s	Hover endurance	5 min

2. Design Methodology

In order to satisfy the above objective, the methodology presented in Ref. [1] and shown in figure 2 are followed.

The first step in the design process is the survey on transitional UAVs with similar design requirements. The output of this survey is a statistical data for different parameters (e.g., maximum take-off weight, payload weight, range, endurance, aspect ratio, span, etc.) that can be considered as a reference for the ranges about which the results should be lie. These statistical data typically presented in the form of curve fitting.

3. Configuration Selection

After collect data from survey and have an estimate about the main features of similar UAVs, the UAV configuration is selected. Typically, each major UAV component may have several alternatives which all may satisfy the design requirements [2]. However, each alternative will have advantages and disadvantages by which the design requirements are satisfied at different levels. Since each design requirement has a unique weight, each alternative result in a different level of satisfaction, and a trade-off analysis technique will be used. The primary impacts of the alternatives of each component are imposed on aerodynamic characteristics and performance/stability in fixed-wing and VTOL flight modes. The comparison between different configurations is performed in Excel sheets, where a free hand sketch for the resulted configuration is shown in figure 3.

It is noted that the tilt rotor UAVs are more suitable and match the design requirements than the other subtypes due to the following reasons: 1) the shafts and nacelles are only required to rotate rotors instead of wings or other heavy structures which saves power and weight; 2) the controllability and stability of tiltrotors in vertical flight when compared to other transitional UAVs.

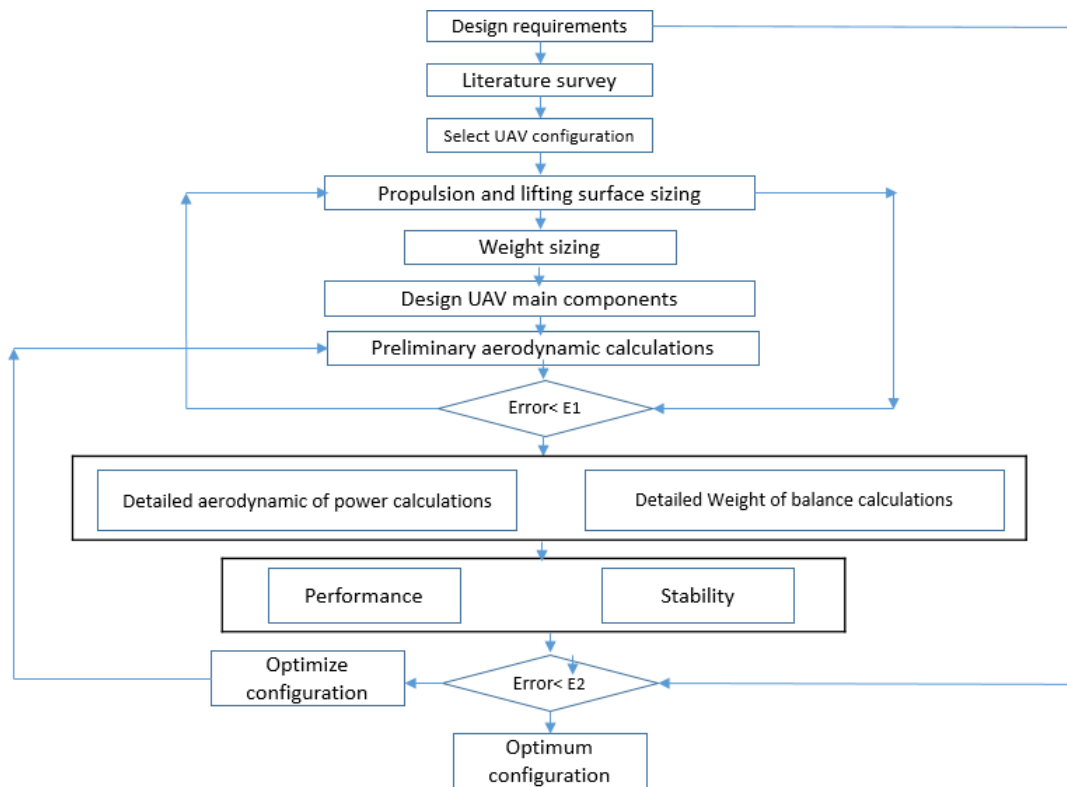


Figure 2. Block diagram for the transitional UAV design procedure.

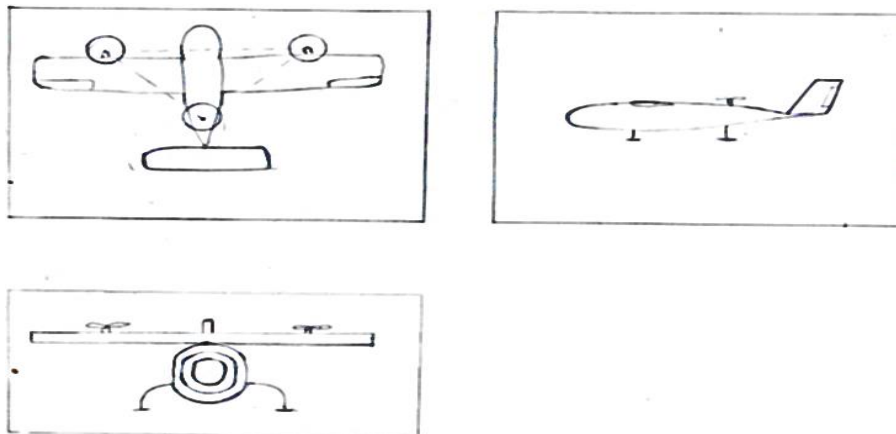


Figure 3. Free-hand sketch for the initial configuration selection.

4. Lifting Surfaces and Propulsion System Sizing

The purpose of this step is to ensure that the tiltrotor UAV will meet the performance requirements in both vertical and horizontal flight modes. Figure 4 summarizes the steps used for the sizing process.

4.1. In horizontal flight mode

The traditional performance equations of fixed-wing (FW) aircraft [4] are used to obtain a relation between wing loading (W/S) and the related power loading (W/P). The following performance requirements are used (stall speed, maximum rate of climb (Roc), ceiling, maximum forward speed).

Any UAV aerodynamic/geometric parameter that is needed in this step is estimated based on the statistical data. The results of this step are shown in figure 5.

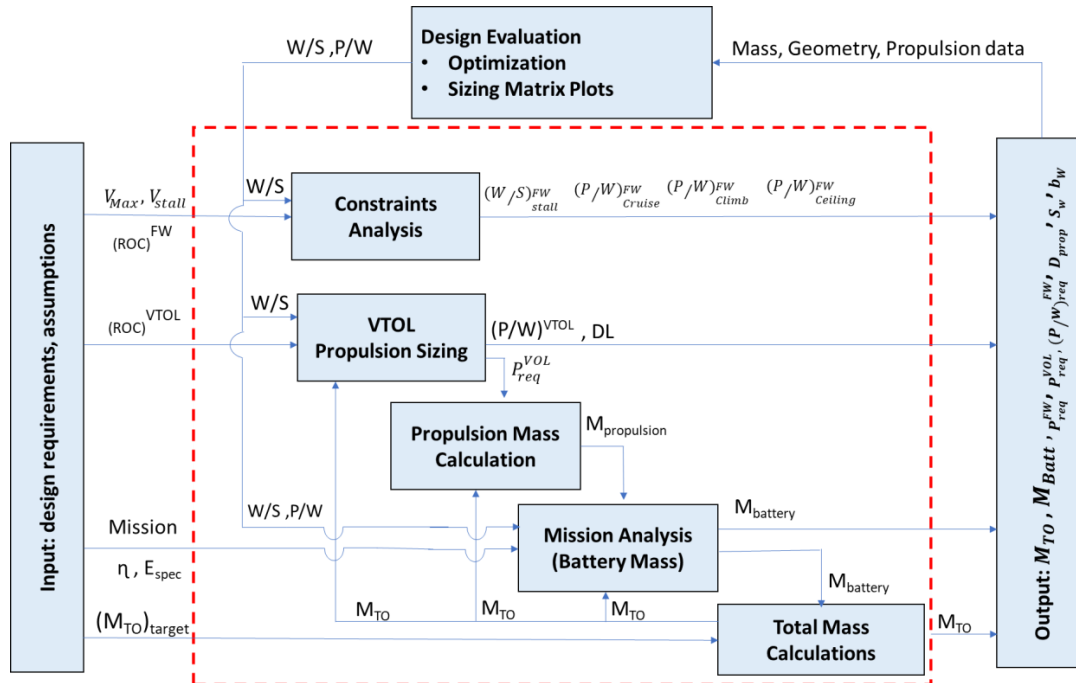


Figure 4. Block diagram for the sizing process.

4.2. In vertical flight mode

The sizing equations and procedure presented in Ref. [4] are used to size the UAV according to the following constraints: (hovering altitude, vertical rate-of-climb, hover ceiling, wingspan limit, transition flight time). Figure 6 shows the results of this step.

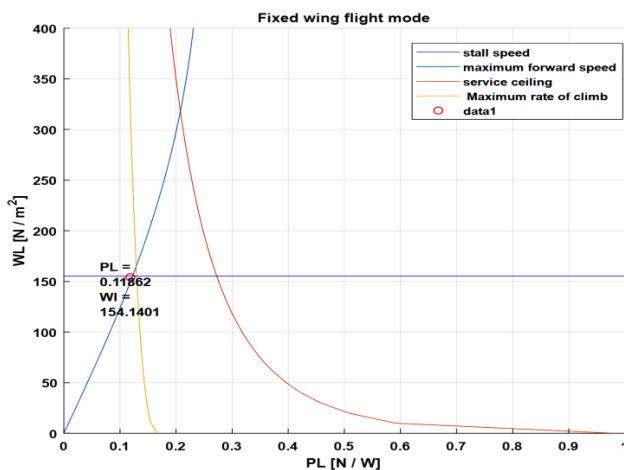


Figure 5. Fixed-wing matching curve.

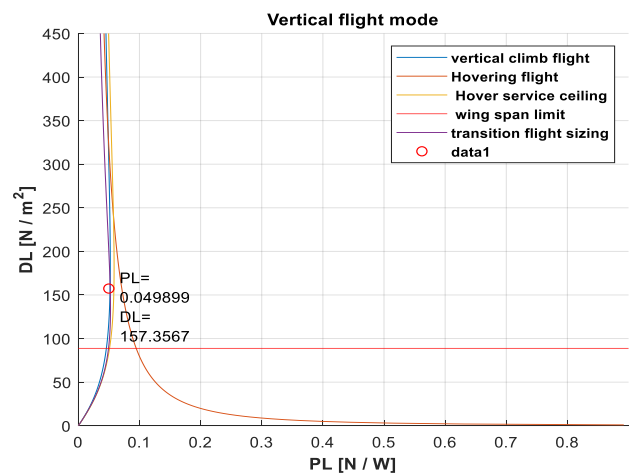


Figure 6. Matching curve in vertical flight mode.

4.3. Weight sizing

The purpose of this section is to get the first estimate of the maximum take-off weight (MTOW) for the tiltrotor UAV before it is designed and built. The value for the MTOW is not final and must be amended in the final design phases. The calculation of this step may have up to about 20% inaccuracies, since it is not based on the real UAV data. But the calculation relies on other UAV statistical data with similar configuration, requirements, and mission. Based on Ref. [1], the UAV weight is broken into several the following parts: payload weight (W_{PL}), propulsion system weight (W_{PS}), battery weight (W_{Batt}), and empty weight minus propulsion system (W_{E-PS}). The method and equations in Ref. [1] are used to obtain the tiltrotor weight sizing and the results are obtained from figure 7. A summary for the lifting surfaces, propulsion, and weight sizing is presented in Table 2.

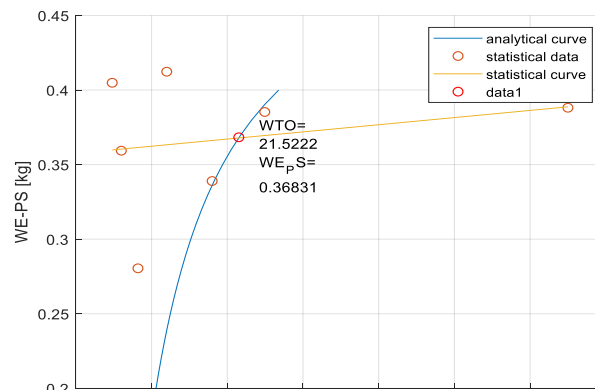


Figure 7. Take-off weight sizing.

Table 2. Outputs of the sizing process

Parameter	Value	Parameter	Value
Take-off mass [kg]	21.5	Empty weight [kg]	9.7
Wing loading [N/m^2]	153.6	Battery weight [kg]	8.2
Wing area [m^2]	1.37	Power loading (FW) [N/W]	0.117
Wing span [m]	3.5	Power loading (VT) [N/W]	0.0498
Maximum lift coefficient [-]	1.5	Wing aspect ratio	9
Maximum power (FW) [W]	1790.1	Maximum power (VT) [W]	4231.2
Rotor disc loading [N/m^2]	157.35		

5. Design of the tiltrotor UAV main components

After sizing process, the initial design for main component of the UAV (i.e., wing, fuselage, horizontal tail, vertical tail, propulsion system, landing gear, and control surfaces) is performed.

For the wing design, the process in Ref [3] and summarized in the flowchart in figure 8 is used to design the tiltrotor wing and the lift distribution along span is calculated and optimized using lifting line theory as presented in figure 10. The designed wing planform is combined wing rectangular at mid and tapered outboard. For the airfoil selection, a weighting process is performed between more than 50 airfoils and the selected airfoil is (S2091-101-83) airfoil that has the aerodynamic characteristics shown in figure 9. For the horizontal and vertical tail, the process shown in figure 11 is followed. Similarly, the empennage airfoils are selected to be symmetric sections with thickness less than wing airfoil thickness. The selected airfoil is (NACA 0008).

For the fuselage design, the procedure shown in figure 12 is used to obtain two major parameters (i.e., fuselage length L_f , maximum diameter D_f).

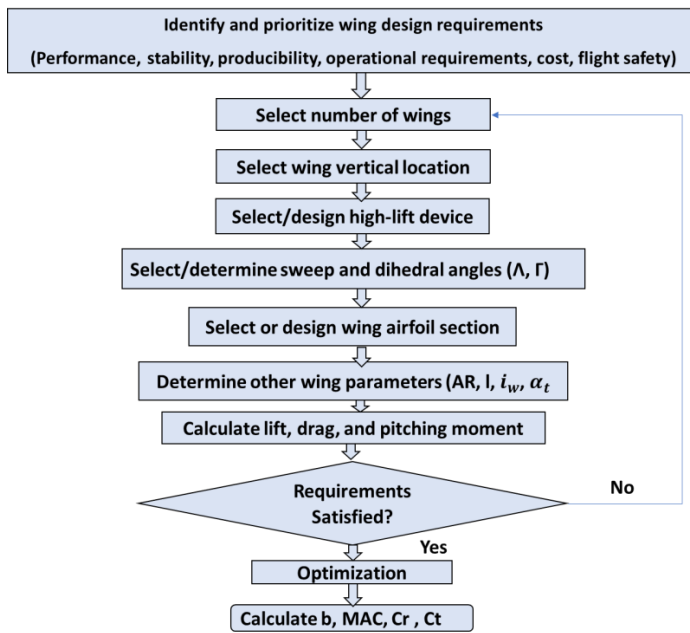


Figure 8. flowchart for wing design process.

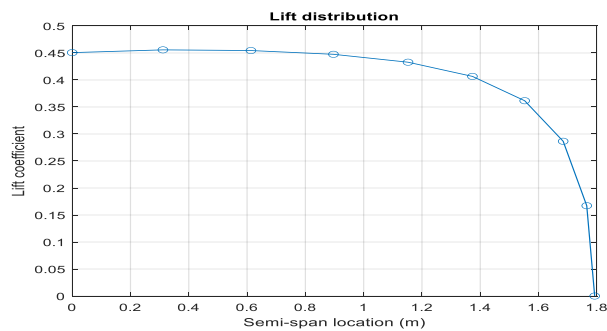


Figure 10. Lift distribution on wing.

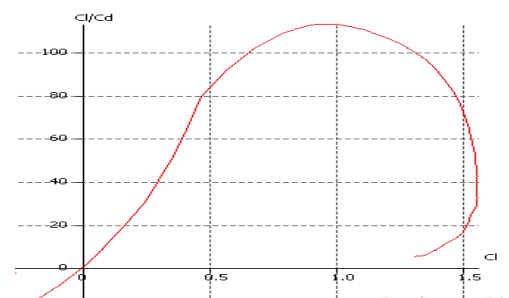
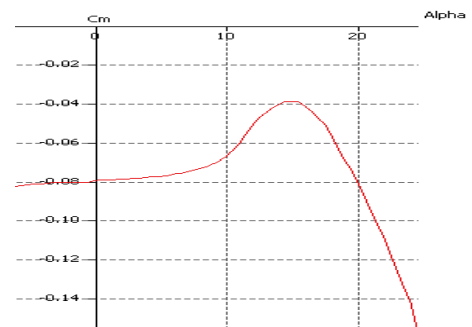
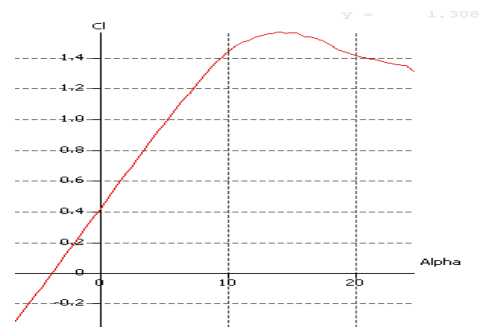


Figure 9. Airfoil aerodynamic characteristics.

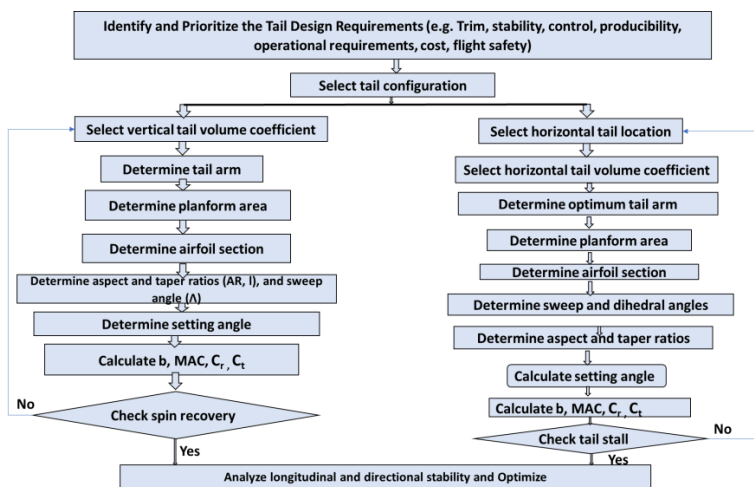


Figure 11. The tail design procedure.

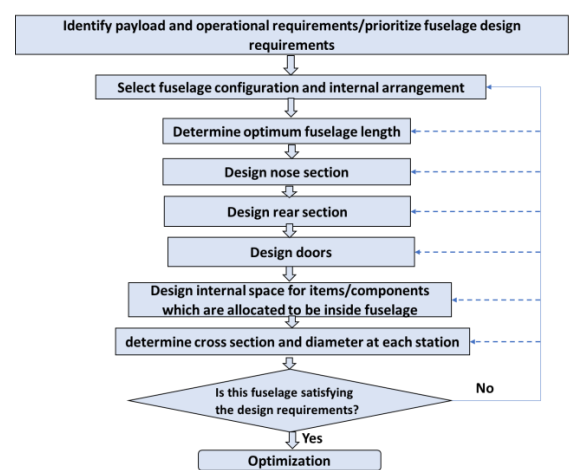


Figure 12. Fuselage design procedure.

6. Detailed Weight Analysis

Typically, the weight analysis of a new designed airplane includes the following three types: 1) Aircraft weight estimation that is based on statistical data and has a typical accuracy of (70–90%); 2) Aircraft weight calculation based on empirical relations to determine the weight of each component and its accuracy ranging between (85–95%); 3) Aircraft weight measurement with approximately 100% accuracy. This section presents the second steps (i.e., weight calculation) for the designed electric tiltrotor UAV. As there is no specific reference that tackle such type of UAVs, six different methods that gathered from various sources (i.e., Ref. [3,7,12]) are used to calculate the weight of the main components and the results are compared in order to assess their accuracy for calculating the weight of electric tiltrotor UAVs.

6.1. Wing weight

For the wing weight calculation, the following expressions estimate the weight of the wing structure including aileron, and flap without the propulsion weight (if it installed at wing). The following methods are used:

6.1.1. Cessna method

$$W_{wCessna} = 0.04674 \cdot (n_z W_o)^{0.397} S_w^{0.360} AR_w^{1.712} \text{ (Cantilever)} \quad (1)$$

6.1.2. Raymer method

$$W_{wRaymer} = 0.036 \cdot S_w^{0.758} W_{FW}^{0.0035} \left(\frac{AR_w}{\cos^2 \Lambda_{c/4}} \right)^{0.6} \cdot q^{0.006} \lambda_w^{0.04} \left(\frac{100 \cdot t/c}{\cos \Lambda_{c/4}} \right)^{-0.3} (n_z W_o)^{0.49} \quad (2)$$

6.1.3. UASF method

$$W_{wUsaf} = 96.948 \left[\left(\frac{n_z W_o}{10^5} \right)^{0.65} \left(\frac{AR_w}{\cos^2 \Lambda_{c/4}} \right)^{0.57} \left(\frac{S_w}{100} \right)^{0.61} \left(\frac{1 + \lambda_w}{2(t/c)} \right)^{0.36} \sqrt{1 + \frac{V_H}{500}} \right] 0.993 \quad (3)$$

6.1.4. Torenbeek method

$$W_{wTorenbeek} = 0.00125 \cdot W_o \left(\frac{b_w}{\cos \Lambda_{c/2}} \right)^{0.75} \left(1 + \sqrt{\frac{6.3 \cos \Lambda_{c/2}}{b_w}} \right) n_z^{0.55} \left(\frac{b_w S_w}{t_{wmax} W_o \cos \Lambda_{c/2}} \right)^{0.30} \quad (4)$$

where: b_w is the wing span in [ft.], S_w is the Trapezoidal wing area [ft^2], AR_w is the Aspect ratio of wing, λ_w is the Taper ratio, $\Lambda_{c/4}$ is the sweep at 25% MGC, $\Lambda_{c/2}$ is the sweep at 50% MGC, W_w is the Predicted weight of wing in lb_f , W_{FW} is the Weight of fuel in wing in (lb_f), q is the Dynamic pressure at cruise (lb_f/ft^2), n_z is the Ultimate load factor (=1.5x limit load factor), W_o is the Design gross weight in (lb_f), V_H is the Maximum level airspeed at S-L in KEAS, t/c is the Wing thickness –to-chord ratio (Maximum), t_{wmax} is the Maximum thickness of the wing root chord in [ft.]

6.1.5. Sedarey method

$$W_{wSadraey} = S_w \cdot MAC \cdot \left(\frac{t}{c} \right)_{max} \rho_{mat} K_p \left(\frac{AR \cdot n_{ult}}{\cos \Lambda_{0.25}} \right)^{0.6} \cdot \lambda^{0.04} \cdot g \quad (5)$$

where: S_w is the wing planform area in [m^2], MAC is the wing mean aerodynamic chord in [m], AR is the aspect ratio, n_{ult} is the Ultimate load factor, $\Lambda_{0.25}$ is the quarter chord sweep angle, λ is the taper ratio, $\left(\frac{t}{c} \right)_{max}$ is the maximum thickness-to-chord ratio, ρ_{mat} is the density of construction material. (Kg/m^3).

6.1.6. Jag Gundlach Method

$$W_{wJag} = F1 \cdot S_w^{E1} \cdot \left[\frac{AR}{\cos^2 \Lambda_{c/4}} \right]^{E3} \cdot q^{E4} \cdot \lambda^{E5} \cdot \left[\frac{t/c_{root}}{\cos \Lambda_{c/4}} \right]^{E6} \cdot (N_z \cdot W_{DG})^{E7} + C1 \quad (6)$$

where: $F1$ is the multiplication factor, $E1$ through $E7$ are exponent factors, $C1$ is an additive constant, N_z is the Ultimate load factor, S_w is the planform area in [m^2], c_{root} is the root chord [m].

6.2. Horizontal tail (HT) Weight

The following methods are used to calculate the weight of the horizontal stabilizer and the elevator.

6.2.1. Cessna method

$$W_{HTCessna} = \frac{3.184W_0^{0.887}S_{HT}^{0.101}AR_{HT}^{0.138}}{174.04t_{HTmax}^{0.223}} \quad (7)$$

6.2.2. Raymer method

$$W_{HTRaymer} = 0.016(n_zW_0)^{0.414}q^{0.168}S_{HT}^{0.896} \left(\frac{100 \cdot t/c}{\cos \Lambda_{C/4}}\right)^{-0.12} \left(\frac{AR_W}{\cos^2 \Lambda_{HT}}\right)^{0.043} \lambda_{HT}^{-0.02} \quad (8)$$

6.2.3. Torenbeek method

The following equation predicts the combined weight of both horizontal and vertical tail.

$$W_{HTTorenbeek} = 0.04[n_z(S_{HT} + S_{VT})^2]^{0.75} \quad (9)$$

6.2.4. USAF Method

$$W_{HTUsaf} = 71.927 \left[\left(\frac{n_zW_0}{10^5}\right)^{0.87} \left(\frac{S_{HT}}{100}\right)^{1.2} \left(\frac{l_{HT}}{10}\right)^{0.483} \sqrt{\frac{b_{HT}}{t_{HTmax}}} \right] 0.458 \quad (10)$$

where: b_{HT} is the HT span in [ft.], S_{HT} is the Trapezoidal HT area [ft^2], AR_{HT} is the Aspect ratio of HT, λ_{HT} is the Taper ratio of HT, Λ_{HT} is the HT sweep at 25% MGC, W_{HT} is the Predicted weight of HT in lb_f , W_0 is the Design gross weight in lb_f , l_{HT} is the Horizontal tail arm in [ft], t_{HTmax} is the maximum thickness of the HT root chord in [ft.], W_{EMP} is the combined Weight of HT and VT in lb_f .

6.2.5. Sedarey method

$$W_{HTSedraey} = S_{HT} \cdot MAC_{HT} \cdot \left(\frac{t}{c}\right)_{maxHT} \cdot \rho_{mat} \cdot K_{\rho HT} \left(\frac{AR_{HT}}{\cos(\Lambda_{0.25HT})}\right)^{0.6} \lambda_{HT}^{0.04} \cdot \bar{v}_H^{0.3} \cdot \left(\frac{C_e}{C_t}\right)^{0.4} \cdot g \quad (11)$$

where: S_{HT} is the HT planform area in [m^2], AR_{HT} is the aspect ratio, $\Lambda_{0.25HT}$ is the HT quarter chord sweep angle, λ_{HT} is the HT taper ratio, $\frac{C_e}{C_t}$ is the elevator-to-tail chord ratio, \bar{V}_H is the HT volume ratio, $K_{\rho HT}$ is the horizontal tail density factor, MAC_{HT} is the HT mean aerodynamic chord in [m], $\left(\frac{t}{c}\right)_{max}$ is the HT maximum thickness-to-chord ratio.

6.2.6. Jag Gundlach Method

$$W_{HTJag} = F_1 \cdot S_{HT}^{E_1} \cdot \left[\frac{AR}{\cos^2(\Lambda_{C/4})}\right]^{E_3} \cdot q^{E_4} \cdot \lambda^{E_5} \cdot \left[\frac{t/c_{root}}{\cos(\Lambda_{C/4})}\right]^{E_6} \cdot [N_z W_{DG}]^{E_7} + C_1 \quad (12)$$

where: F_1 is the multiplication factor, E_1 through E_7 are the exponent factors, C_1 is an additive constant, N_z is the Ultimate load factor, S_{HT} is the HT planform area in [m^2], c_{root} is the HT root chord [m].

6.3. Vertical tail (VT) Weight

The expressions below predict the weight of the VT.

6.3.1. Cessna method

The Cessna equation is valid for $V_H < 200$ KTAS.

$$W_{VTcessna} = (1 + 0.2F_{tail}) \frac{1.68W_0^{0.567}S_{VT}^{0.1249}AR_{VT}^{0.482}}{639.95t_{VTmax}^{0.747}(\cos \Lambda_{VT})^{0.882}} \quad (13)$$

6.3.2. Raymer method

$$W_{VT\text{Raymer}} = 0.073(1 + 0.2F_{tail})(n_z W_0)^{0.376} q^{0.122} S_{VT}^{0.873} \left(\frac{100 \cdot t/c}{\cos \Lambda_{VT}}\right)^{-0.49} \left(\frac{AR_W}{\cos^2 \Lambda_{VT}}\right)^{0.357} \lambda_{VT}^{0.039} \quad (14)$$

6.3.3. Torenbeek method

$$W_{HT\text{Torenbeek}} = 0.04[n_z(S_{HT} + S_{VT})^2]^{0.75} \quad (15)$$

6.3.4. USAF Method

$$W_{VT\text{Usaf}} = 55.786(1 + 0.2F_{tail}) \left[\left(\frac{n_z W_0}{10^5}\right)^{0.87} \left(\frac{S_{VT}}{100}\right)^{1.2} \sqrt{\frac{b_{VT}}{t_{VT\text{max}}}} \right]^{0.458} \quad (16)$$

where: b_{VT} is the VT span in [ft.], S_{VT} is the Trapezoidal VT area [ft^2], AR_{VT} is the Aspect ratio of VT, λ_{VT} is the Taper ratio of VT, Λ_{VT} is the VT sweep at 25% MGC, W_{VT} is the Predicted Weight of VT in lb_f, W_0 is the Design gross weight in lb_f, $F_{tail}=0$, for conventional tail, =1 for T-tail, $t_{VT\text{max}}$ is the Maximum thickness of the VT root chord in [ft.]

6.3.5. Sedarey method

$$W_{VT\text{Sedraey}} = S_{VT} \cdot MAC_{VT} \cdot \left(\frac{t}{c}\right)_{\text{maxVT}} \cdot \rho_{\text{mat}} \cdot K_{\rho VT} \left(\frac{AR_{VT}}{\cos(\Lambda_{0.25VT})}\right)^{0.6} \lambda_{HT}^{0.04} \cdot \bar{v}_V^{0.2} \cdot \left(\frac{C_r}{C_v}\right)^{0.4} \cdot g \quad (17)$$

where: S_{VT} is the VT planform area in [m^2], MAC_{VT} is the VT mean aerodynamic chord in [m], AR_{VT} is the aspect ratio, $\Lambda_{0.25VT}$ is the VT quarter chord sweep angle, λ_{VT} is the VT taper ratio, $\frac{C_r}{C_v}$ is the rudder-to-tail chord ratio, \bar{v}_V is the HT volume ratio, $K_{\rho VT}$ is the horizontal tail density factor.

6.3.6. Jag Gundlach Method

$$W_{VT\text{Jag}} = F_1 \cdot S_{VT}^{E_1} \cdot \left[\frac{AR}{\cos^2(\Lambda_{C/4})}\right]^{E_3} \cdot q^{E_4} \cdot \lambda^{E_5} \cdot \left[\frac{t/c_{root}}{\cos(\Lambda_{C/4})}\right]^{E_6} \cdot [N_z W_{DG}]^{E_7} + C_1 \quad (18)$$

where: F_1 is the multiplication factor, E_1 through E_7 are the exponent factors, C_1 is an additive constant, N_z is the Ultimate load factor, S_{VT} is the VT planform area in [m^2], c_{root} is the VT root chord [m].

6.4. Fuselage Weight

The following expressions predict the weight of the fuselage shell and the associated internal structure

6.4.1. Cessna method

Note that Cessna equation is valid only for $V_H < 200$ KTAS, For UAV put $N_{occ}=1$.

$$W_{Fus\text{Cessna}} = 14.86 W_0^{0.144} \left(\frac{l_{FS}}{R_{\text{max}}}\right)^{0.778} l_{FS}^{0.383} N_{occ}^{0.445} (\text{for high wing}) \quad (19)$$

6.4.2. Raymer method

$$W_{Fus\text{Raymer}} = 0.052 S_{FUS}^{1.086} (n_z W_0)^{0.177} l_{HT}^{-0.051} \left(\frac{l_{FS}}{d_{FS}}\right)^{-0.072} q^{0.241} + 11.9 (V_p \Delta P)^{0.271} \quad (20)$$

6.4.3. USAF Method

$$W_{Fus\text{Usaf}} = 200 \left[\left(\frac{n_z W_0}{10^5}\right)^{0.87} \left(\frac{l_f}{10}\right)^{0.857} \left(\frac{w_f + d_f}{10}\right) \left(\frac{V_H}{100}\right)^{0.332} \right]^{1.1} \quad (21)$$

where: W_{FUS} is the Predicted fuselage weight in lb_f, S_{FUS} is the Fuselage wetted area. ft^2 , d_f is the Fuselage max depth in [ft], d_{FS} is the Depth of fuselage structure in [ft], V_p is the Volume of pressurized cabin in [ft^3], l_f is the Fuselage length in [ft]. l_{FS} is the Length of fuselage structure in [ft], R_{max} is

the fuselage maximum perimeter in [ft], N_{OCC} is the Number of occupants (crew& passengers), ΔP is the cabin pressure differential in [psi].

6.4.4. Sedarey method

$$W_{FusSedarey} = L_f \cdot D_{fmax}^2 \cdot \rho_{mat} \cdot K_{\rho F} \cdot n_{ult}^{0.25} \cdot K_{inlet} \cdot g \quad (22)$$

where: L_f is the fuselage length in [m], D_{fmax} is the fuselage maximum diameter of the equivalent circular cross-section in [m], ρ_{mat} is the density of construction material in (Kg/m^3), $K_{\rho F}$ is the fuselage density factor (0.002-0.003) for home built, $K_{inlet}=1.25$ for the case of inlets on the fuselage, and 1 for inlets elsewhere.

6.4.5. Jag Gundlach Method

A general fuselage structural weight equation for a semi-monocoque structure or composite shell fuselage in subsonic or transonic UAVs are given by the following equation.

$$W_{FusJag} = 0.5257 \cdot F_{MG} \cdot F_{NG} \cdot F_{press} \cdot F_{VT} \cdot F_{Matl} \cdot L_{struct}^{0.3796} \cdot (W_{carried} \cdot N_Z)^{0.4863} \cdot V_{Eqmax}^2 \cdot lb \quad (23)$$

where: L_{struct} is the structural length of the fuselage in [ft], N_Z is the load factor in [g], V_{Eqmax} is the maximum equivalent velocity in [knots], $W_{carried}$ is the weight of the components carried within the structure in [pounds], the (F) parameter definitions and values are detailed in Table 3.

Table 3. Parameter Definitions and Values

Term	Definition	Value
F_{MG}	Main gear on the fuselage factor	=1 (if not fixed on fuselage), =1.07 (if fixed fuselage)
F_{NG}	Nose gear on the fuselage factor	=1 (if not fixed on fuselage), =1.04 (if fixed on fuselage)
F_{press}	Pressurized fuselage factor	=1 (for unpressurized), =1.08 (for pressurized)
F_{VT}	Vertical tail on the fuselage factor	=1 (if VT weight not included), =1.1 (if VT weight included)
F_{Matl}	Materials factor	=1 (for carbon-fiber), =2 (for fiberglass), =1 (for metal), =1.187 (for wood), =2 (for others).

6.5. Propulsion System Weight

The following approaches are used to calculate the weight of the engine with nacelles or cowling and propellers.

6.5.1. Cessna method

$$W_{EI\ Cessna} = (1.3P_{mx} + W_{prop})N_{ENG} + W_{NAC} \quad (24)$$

6.5.2. Raymer method

$$W_{EI\ Raymer} = 2.575W_{ENG}^{0.992}N_{ENG} \quad (25)$$

6.5.3. Torenbeek method

$$W_{EI\ Torenbeek} = (W_{ENG} + W_{Prop})N_{ENG} + 1.03N_{ENG}^{0.3}P_{max}^{0.7} + W_{NAC} \quad (26)$$

6.5.4. USAF Method

$$W_{EI\ Usaf} = 2.575W_{ENG}^{0.922}N_{ENG} \quad (27)$$

where: W_{EI} is the predicted weight of all installed engines in [lb_f], W_{ENG} is the Weight of each uninstalled engine in [lb_f], W_{Prop} is the Weight of a single propeller in [lb_f]

6.5.5. Sedarey method

$$W_{Ps\ Sedraey} = K_E \cdot N_E \cdot (W_E)^{0.9} \quad (28)$$

where: N_E is the number of engines, K_E is the engine weight factor.

6.5.6. Jag Gundlach Method

$$W_{PropJag} = W_{Engine} + W_{Props} + W_{nac} + W_{ESC} \quad (29)$$

where: W_{Engine} is the electric motor weight and can be obtained from the following equation:

$$\frac{W_{Motor}}{P_{Mot,max}} = F1 \times P_{Mot,max}^2 \times V_{Max}^2 \quad (30)$$

As $F1$ is a constant, $E1$ and $E2$ are exponents, P_{Max} is the maximum output power of the motor [watt], and V_{Max} is the maximum rated motor voltage.

For the weight of propellers, W_{prop} can be calculated as per the following equation:

$$W_{prop} = K_{prop} N_{props} N_{blade}^{0.391} \left(\frac{D \cdot P_{Max}}{1000 \cdot N_{props}} \right)^{0.782} [lb] \quad (31)$$

As K_{prop} is a multiplication factor, N_{props} is the number of propellers (assumed to be equal to the number of engines), D is the propeller diameter in [ft], P_{Max} is the total maximum shaft horsepower of all engines, and N_{blades} is the number of blades for each propeller. Roskam recommends K_{prop} value of 24.0 for turboprops above 1,500 hp and 31.92 for engines below 1,500 hp. In this work, K_{prop} value of 15 is recommended for plastic or composite propellers for engines with less than 50 hp.

For the nacelles weight, W_{nac} can be calculated from the following equation:

$$W_{nac} = F_{nac} \cdot T_{max} [lb] \quad (32)$$

where: T_{max} is the maximum thrust of all engines.

Finally, the electronic speed controller weight, W_{ESC} , is calculated by the following equation:

$$W_{ESC} = F_{ESC} \cdot P_{Mot,Max} \quad (33)$$

where: F_{ESC} approximately 0.08 lb/kW for brushed and brushless motors

6.6. conclusion

The detailed weight of the tiltrotor main components is calculated from above empirical equations, and the data are averaged (using the reasonable results only, compared with statistical data) for each UAV component, and these data are collected in Table 4. It is noted that for small UAVs, Cessna method is inadequate in calculating the wing weight. Additionally, both Raymer and Cessna methods are inadequate in calculating the fuselage weight.

Resizing process

After determining the detailed weight of the main UAV components and having more details about the final shape of the UAV, a resizing process is performed and the obtained results are presented in Table 5. After determine the output of the resizing process, both batteries, motors (tilting and tail), and propellers can be selected.

7. Weight and Balance

Typically, the distribution of the UAV weight influences the airworthiness and performance via two parameters: 1) UAV center of gravity (cg), 2) UAV mass moment of inertia. This section presents the calculation procedure for these important parameters.

Table 4. Detailed weight of different UAV components

Detailed Weight Estimation									
Components/ Different methods	Raymer method	USAF method	Cessna Method	Torenbek method	Sedarey method	Jay Gundlach method	Average	Initial weight Estimation	Error %
Wing [Kg]	3.064	1.821	18.037	1.598	1.889	1.377	1.950		
Horizontal tail [Kg]	0.351	0.727	0.654	0.398	0.130	0.664	0.487		
Vertical tail [Kg]	0.384	0.338	0.149	0.398	0.072	0.498	0.307		
Fuselage [Kg]	6.716	-	6.381	1.648	1.899	3.702	2.416		
Landing gear	-	-	-	-	-	-	0.500		
Engines + Tilting mechanism [Kg]	3.481	4.185	4.392	3.333	4.387	2.206	3.332	2.014	-65.41
Batteries [Kg]	-	-	-	-	-	-	9.000	9.000	
Avionics [Kg]	-	-	-	-	-	-	0.500		
Payload [Kg]	-	-	-	-	-	-	3.500	3.500	
Skin [Kg]	-	-	-	-	-	-	0.500		
Adhesive materials [Kg]	-	-	-	-	-	-	0.500		
(Empty - propulsion) weight [Kg]	-	-	-	-	-	-	7.160	8.980	20.270
Total weight [Kg]							22.992	23.500	2.162

Table 5. Output of resizing process

Parameter	Value	Parameter	Value
Take-off mass [kg]	23.59	Empty weight [kg]	11.3
Wing loading [N/m ²]	153.6	Battery weight [kg]	9.26
Wing area [m ²]	1.53	Power loading (FW) [N/W]	0.1166
Wing span [m]	3.6	Power loading (VT) [N/W]	0.0493
Maximum lift coefficient [-]	1.5	Wing aspect ratio	9
Maximum power (FW) [W]	2015	Maximum power (VT) [W]	4766
Rotor disc loading [N/m ²]	160.23		

7.1. Aircraft center of gravity (cg)

Center of gravity determined from the following relations:

$$X_{cg} = \frac{\sum_{i=1}^n W_i x_{cg_i}}{\sum_{i=1}^n W_i} = \frac{\sum_{i=1}^n m_i x_{cg_i}}{\sum_{i=1}^n m_i} \quad (34)$$

$$Y_{cg} = \frac{\sum_{i=1}^n W_i y_{cg_i}}{\sum_{i=1}^n W_i} = \frac{\sum_{i=1}^n m_i y_{cg_i}}{\sum_{i=1}^n m_i} \quad (35)$$

$$Z_{cg} = \frac{\sum_{i=1}^n W_i z_{cg_i}}{\sum_{i=1}^n W_i} = \frac{\sum_{i=1}^n m_i z_{cg_i}}{\sum_{i=1}^n m_i} \quad (36)$$

where, w_i denotes the weight of each aircraft component, m_i denotes the mass of each aircraft component, and x_{cg_i} , y_{cg_i} , and z_{cg_i} the coordinates of each individual component. The coordinates are measured with respect to a particular reference line. The selection of the reference lines is arbitrary, and does not affect the final result.

7.1.1. Longitudinal Center of Gravity Location

The range of CG along the x-axis is the most significant one. The longitudinal cg position is not only influencing the longitudinal (control, stability, trim, handling qualities) and take-off and landing performance, but also greatly affects the elevator design.

It is convenient to express the aircraft cg as a percentage of the Mean Aerodynamic chord (MAC).

$$h = \bar{x}_{cg} = \frac{X_{cg} - X_{LEMAC}}{\bar{c}} \quad (37)$$

For a statically longitudinally stable airplane, the most aft location of the cg must be forward of the neutral point. Thus, the CG location will directly influence longitudinal static stability. The static margin (SM) is defined as the non-dimensional difference between the airplane center of gravity and the airplane neutral point:

$$SM = \frac{X_{np} - X_{cg}}{\bar{c}} \quad (38)$$

The static margin (SM) is selected to be about 15% from mean aerodynamic chord for this category of UAVs.

7.2. Aircraft Mass Moment of Inertia

The moment of inertia around any axis can be calculated from the moment of inertia around the parallel axis that passes through the center of mass. The equation to calculate this is called the parallel-axis theorem, and is given as

$$I_o = I_c + md^2 \quad (39)$$

The mass moment of inertia about each axis is determined from the following equations

$$I_{xx} = I_{xxCG} + m(y^2 + z^2) \quad (40)$$

$$I_{yy} = I_{yyCG} + m(x^2 + z^2) \quad (41)$$

$$I_{zz} = I_{zzCG} + m(y^2 + x^2) \quad (42)$$

$$I_{xz} = I_{xzCG} + mxz \quad (43)$$

7.3. Results of Cg and moment of inertia

The results of the cg and moments of inertia calculations are presented in the Table 6, where X_{cg} is measured from the MAC leading edge.

Table 6. Results of Cg and moment of inertia

Parameter	Value	Parameter	Value
X_{cg}	0.151	I_{xx}	3.725
Y_{cg}	0	I_{yy}	5.617
Z_{cg}	-0.084	I_{zz}	9.139
		I_{xz}	-0.177

8. Control Surfaces Design

The process followed in this paper to design the UAV main control surfaces (i.e., elevator, aileron, and rudder) is summarized in figure 13, where the results of control surface design are summarized in Table 7.

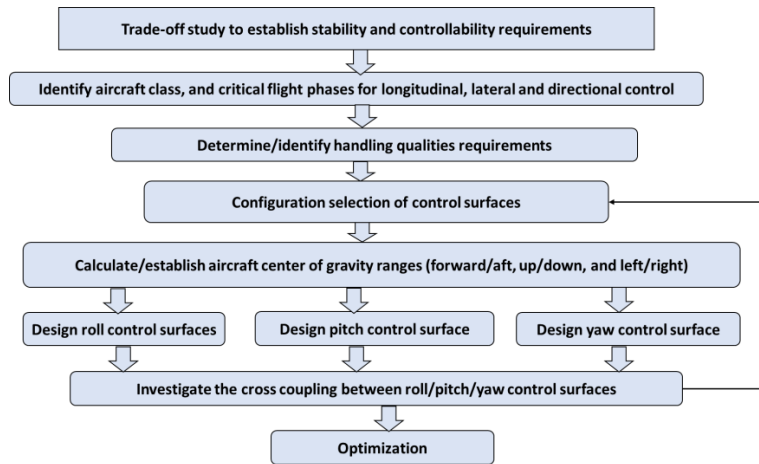


Figure 13. Control surfaces design process.

Table 7. Control surface parameters

Parameter	Value
Aileron span [m]	1.104
Rudder span[m]	0.4
Aileron area [m^2]	0.1151
δ_{Rmax} [deg]	30
δ_{Amax} [deg]	20
Elevator span[m]	1.02
Elevator area [m^2]	0.08874
Rudder area [m^2]	0.0348
δ_{Emax} [deg]	25

9. Detailed Aerodynamics and Mechanics of Flight Analysis in FW Mode

After the design and selection of each UAV component, the aerodynamic analysis is performed to calculate the important UAV characteristic curves and to determine the longitudinal, lateral, and directional aerodynamic derivatives. This process is performed by the following two aerodynamic tools: 1) XFLR5; 2) Digital DATCOM.

9.1. XFLR5 software

To analyze the UAV on the XFLR5, the complete geometric model of the UAV is developed and all airfoils are defined together with the cg and flight conditions. Figure 14 presents a screenshot of the XFLR5 analysis process, whereas some of the important outputs from XFLR5 are shown in figure 15.

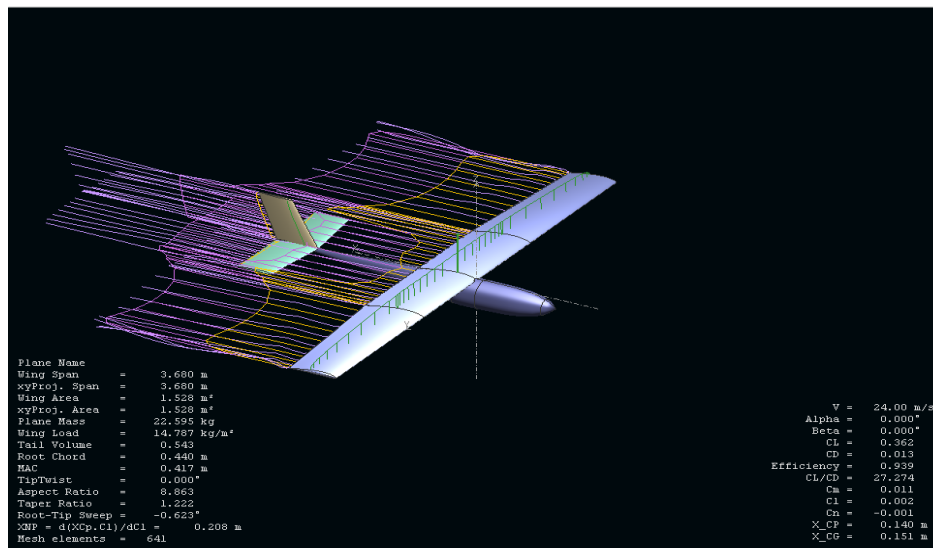


Figure 14. Screenshot of the XFLR5 analysis.

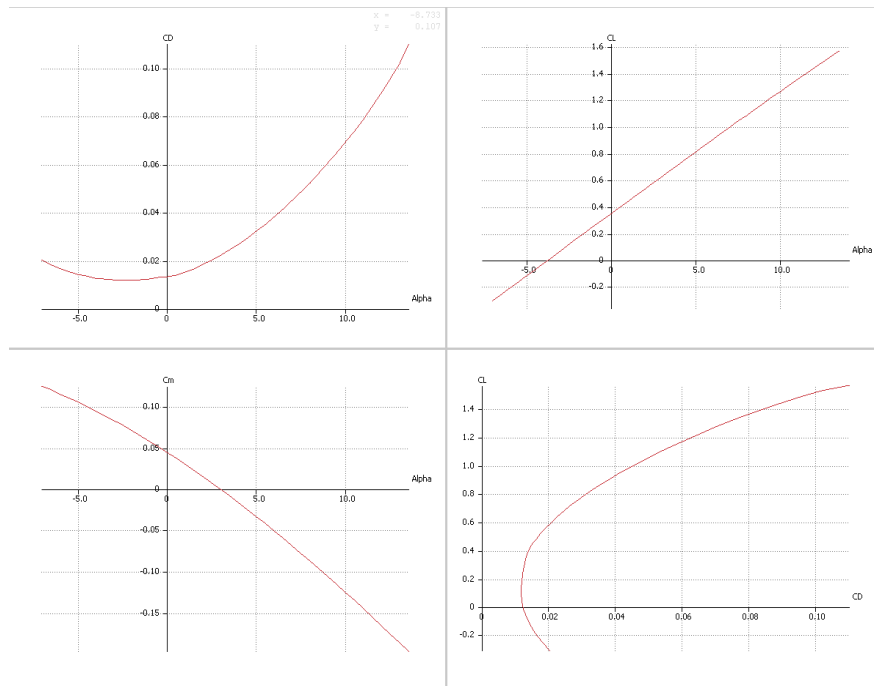


Figure 15. Aerodynamic characteristics of the designed UAV using XFLR5.

9.2. Digital DATCOM

A detailed aerodynamic analysis is performed using the digital DATCOM, where some of the important aerodynamic outputs are illustrated in figure 16.

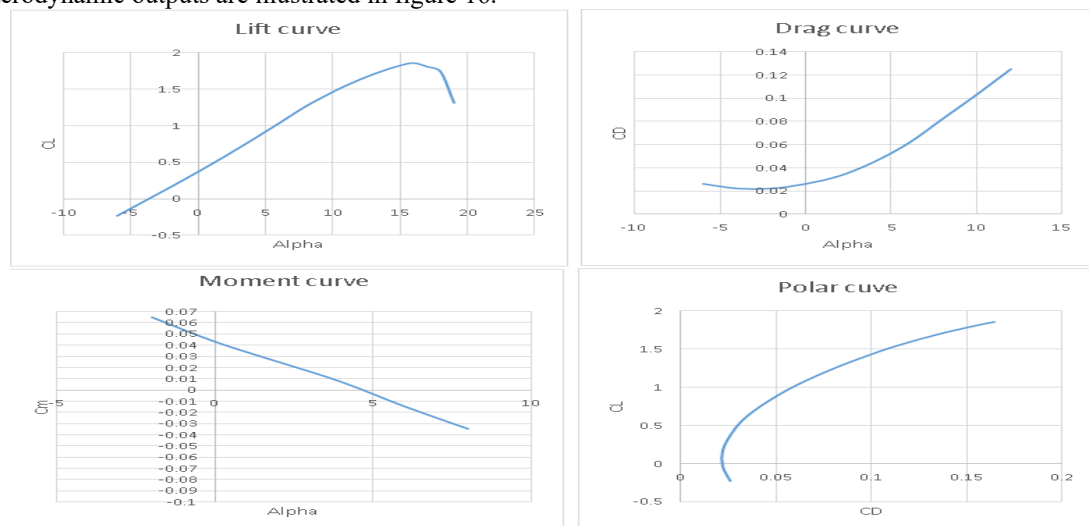


Figure 16. UAV characteristic curves from Datcom software

9.3. Performance Analysis

The performance of the designed tiltrotor UAV is calculated for the three flight modes (i.e., rotorcraft, transition, and fixed-wing) and then compared with the initial design requirements. All necessary equations for calculation the performance are obtained from references [1,2,4,10]. The results showed that all design requirements are satisfied (or even exceeded), except the endurance in hover and fixed-

wing flight modes where the errors are 10% and 20%, respectively. Some of the important fixed-wing performance curves in vertical and horizontal flights are presented in figure 17 and figure 18. From the flight equilibrium diagram (figure 17), the minimum and maximum speeds due to propulsion in level flights can be obtained. Additionally, the speeds corresponding to minimum drag, maximum endurance, maximum rate-of-climb, and maximum range can be obtained.

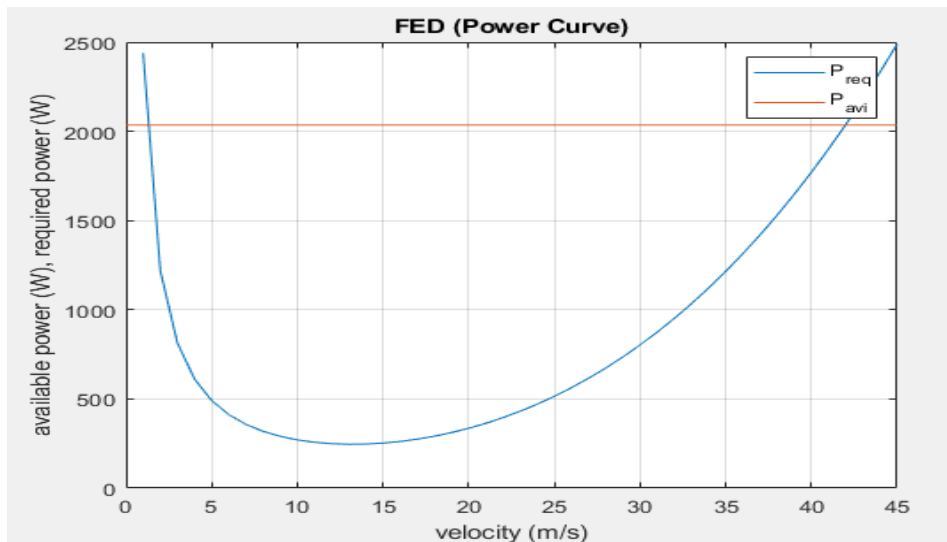


Figure 17. Flight equilibrium diagram at sea-level.

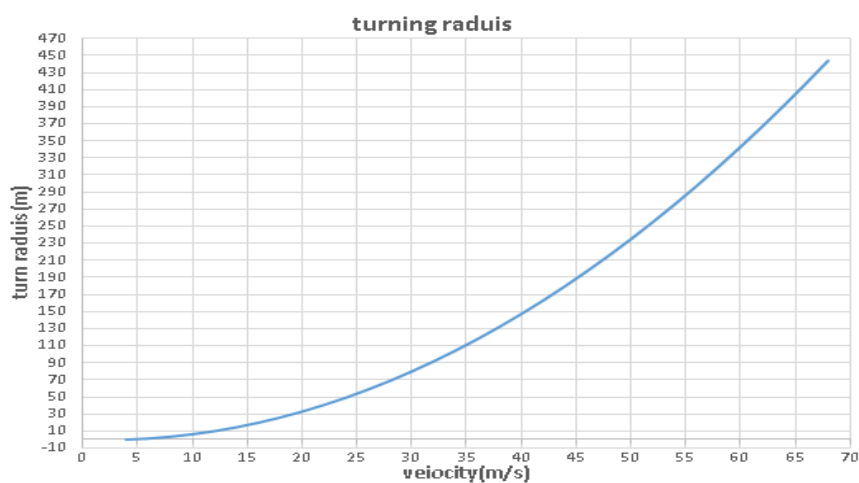


Figure 18. Turn radius versus Velocity at cruise altitude.

9.4. Dynamic Stability Analysis

Studying the dynamic stability means studying the uncontrolled motion of the UAV. The objective is to make the small disturbance properties of the longitudinal and lateral direction motions (the natural modes) to be within the acceptable small values. Based on the aerodynamic coefficient and derivatives that are calculated from the Datcom, and using the equations in Ref [10], the dynamic stability of the designed UAV in longitudinal and lateral-directional modes are analyzed as given in the following subsections.

Longitudinal modes

1. $\lambda_{1,2} = n_1 \pm iw_1$ (n_1 is small, lightly damped, and w_1 is small). This mode is called the “phugoid mode”, where: $\lambda_{1,2} = -0.0003 \pm 0.004i$.
2. $\lambda_{3,4} = n_2 \pm iw_2$ (n_2 large, lightly damped and w_2 is large). This mode is called the “short period mode”, where: $\lambda_{3,4} = -0.0473 \pm 0.0423i$.

Lateral-Directional modes

1. Very slow mode, so the pilot/autopilot can control the UAV even if it is unstable “Spiral mode” where: ($\lambda_1 = 0.0021$).
2. $\lambda_2 = n_2$ (n_2 heavily damped and very rapid). This mode is called the “Rolling mode” where: ($\lambda_2 = -1.13$).
3. $\lambda_{3,4} = n_3 \pm iw_3$ (lightly moderate damped oscillatory mode). This mode is called the “Dutch roll mode” where: $\lambda_{3,4} = -0.0215 \pm 0.146i$

Dynamic Stability Results

A summary of the results of the dynamic stability analysis is presented in Table 8.

Table 8. Stability results

Comparison	Period: \hat{T} [sec]	\hat{t}_{half} [sec]	N_{half}
phugoid mode	13.646	20.074	1.47
short period mode	1.29	0.127	0.0897
spiral mode	–	$t_{double} = 25.3$	–
Roll mode	–	0.047	–
Dutch-roll mode	3.2971	2.47	0.749

10. Preliminary Internal Configuration Design and Assembly

The internal structure of the main components of the tiltrotor UAV is preliminary designed, where the internal structure of the wing is designed to be a spar semi-monocoque structure with main and auxiliary carbon fiber spars and plywood/balsa-wood ribs. Similarly, the horizontal and vertical tail internal structure are spar semi-monocoque structure. The fuselage internal structure design depends also on spar semi-monocoque structure as it contains bulkheads from ply and balsa wood and main boom from carbon fiber connecting all bulkheads to each other. The complete assembly of the tiltrotor UAV internal structure is presented in figure 19.

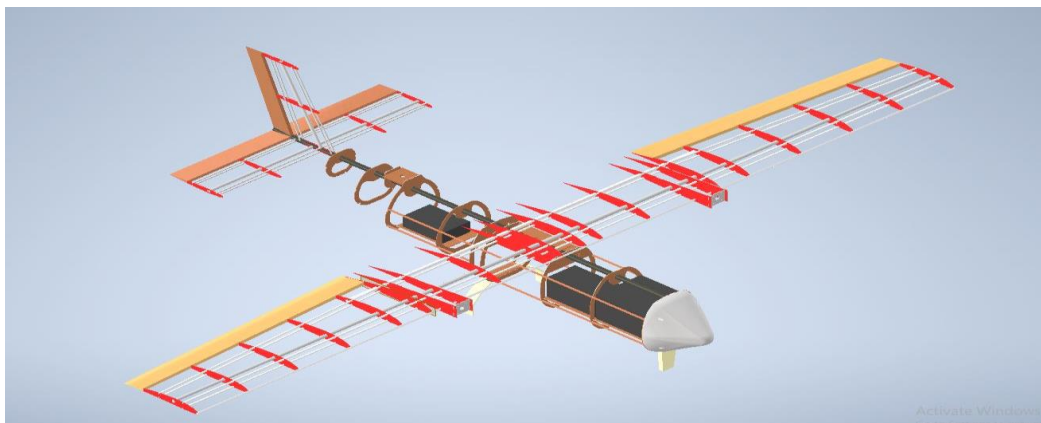


Figure 19. Full assembly of UAV

Conclusion

In this paper, a methodology for designing an electric convertiplane UAV is presented. The configuration is selected to be a tiltrotor UAV based on the design requirements. Performance constraints are developed for the rotorcraft, fixed-wing flight, and transition modes to develop the matching curve charts. This curve enables selecting the best preliminary design parameters via obtaining the satisfactory values of the wing, power, and rotor disc loadings that are needed to fulfil the design requirements in the three modes. A detailed weight and balance analysis is performed, then a resizing process is conducted to update the parameters of the UAV using information about designed/selected parts. A detailed aerodynamic, performance, and stability analysis is performed for the designed tiltrotor UAV. Finally, the internal structure of the UAV is preliminary designed. Future work will include the detailed structure design and analysis, manufacturing, flight testing of the designed tiltrotor UAV.

References

- [1] Kamal A and Ramirez-Serrano A 2020 *AIAA Scitech Forum* p 1733.
- [2] Kamal A M and Ramirez-Serrano A 2020 *Journal of Aircraft* **57**(1) 179-197.
- [3] Sadraey M H 2012 *Aircraft design: A systems engineering approach* (John Wiley & Sons).
- [4] Kamal A M and Ramirez-Serrano A 2019 *Journal of Aircraft* **56**(5) 2083-2092.
- [5] Saeed A S, Younes A B, Cai C and Cai G 2018 *Progress in Aerospace Sciences* **98** 91-105.
- [6] Tyan M, Van Nguyen N, Kim S and Lee J W 2017 *Aerospace Science and Technology* **71** 30-41.
- [7] Raymer D 2012 *Aircraft design: a conceptual approach* (American Institute of Aeronautics and Astronautics, Inc).
- [8] Gudmundsson S 2013 *General aviation aircraft design: Applied Methods and Procedures* (Butterworth-Heinemann).
- [9] Roskam, J 1985 *Airplane Design: Preliminary configuration design and integration of the propulsion system* (DARcorporation).
- [10] Etkin B and Reid L D 1995 *Dynamics of flight: stability and control* (John Wiley & Sons).
- [11] Sadraey M H 2017 *Aircraft performance: an engineering approach* (CRC Press).
- [12] Gudmundsson S 2021 *General Aviation Aircraft Design: Applied Methods and Procedures Ed. 2.* (Elsevier Science).